

Multi-objective optimisation of viscoelastic damping inserts in honeycomb sandwich structures [☆]

P. Aumjaud^a, J.E. Fieldsend^a, M.-A. Boucher^a, K.E. Evans^a, C.W. Smith^{a,*}

^aCollege of Engineering, Mathematics and Physical Sciences, University of Exeter, Exeter EX4 4QF, UK.

Abstract

The Double-Shear Lap Joint (DSLJ) is a novel damping insert sited internally within a structure which is particularly well suited for lightweight sandwich structures with internal voids, such as honeycomb core sandwich panels. In high performance lightweight structures, the insertion of relatively more dense dampers of any type may increase the total mass substantially and alter the mass distribution significantly. The objective herein was to determine the optimum location, number and orientation of DSLJ inserts within a typical sandwich panel, and thereby to assess the efficacy of two different optimisation approaches to this problem; a parametric optimisation and the Adaptive Indicator-Based Evolutionary Algorithm (IBEA). Both approaches were used to maximise the damping while minimising the additional mass of the damping inserts applied to the structure. Although the parametric approach was faster and easier to implement, the Adaptive IBEA identified significantly better configurations in many cases, especially where veering occurred, in one case improving modal loss factors more than fourfold *vs* the parametric method. Solutions were identified with large increases in modal loss factors but only small increases in mass *vs* the empty structure.

Keywords: vibration, damping, sandwich panel, optimisation, lightweight

1. Introduction

Sandwich structures are extensively used in the aerospace and other transport sectors for their low density and excellent mechanical properties [1, 2]. They exhibit a high stiffness-to-mass and strength-to-mass ratios which make them ideal candidates for load-bearing applications where mass is a critical issue. However, structures used in transport are often deployed in vibration-rich environments which leads to high cycle fatigue (and thus more frequent service intervals) and passenger discomfort. Vibration damping in sandwich structures has therefore been the subject of multiple research projects [3]. Initial attempts at designing damped sandwich structures consisted of two rigid skins constraining a monolithic viscoelastic core, i.e. no honeycomb or other stiff core [4, 5]. Although these structures were capable of damping flexural vibration significantly, they were not very weight efficient.

Subsequently, Nokes and Nelson [6] proposed a partial constrained layer damper arrangement which covered only a fraction of the vibrating host structure, and coincidentally was more mass efficient. A later development of this concept was to combine viscoelastic materials with cellular

solids in sandwich cores, in order to provide both significant energy dissipation and good mechanical integrity. Michon et al. [7] filled the cell of a honeycomb-cored sandwich beam with viscoelastic hollow particles which achieved a substantial damping with a moderate impact on the structure's mass and stiffness. Murray et al. [8] proposed filling the cells of a metallic honeycomb structure with a lossy polymer (with a low modulus typical of rubbers) which significantly increased the structural loss factor. Boucher et al. [9] showed that a partial filling of the honeycomb cell void can achieve an appreciable damping, and importantly with only a minimal increase in mass. Recently, the authors developed a new concept – the Double Shear Lap Joint (DSLJ) damper – a high weight-efficiency passive damper which can be located internally within structures, e.g. a honeycomb core [10]. It consists of a double shear lap-joint arrangement which can be inserted along three different orientations into the hexagonal cell of a honeycomb lattice and filled with viscoelastic damping polymer [11].

Development of dampers in general has required use of heuristic optimisation strategies for location, orientation and sizing of the dampers, so as to maximise the modal loss factor of the vibrating structures while minimising the additional mass. Minimising mass and maximising modal loss would normally be competing objectives. In particular, the optimal design of constrained layer dampers, including the number of plies, the ply thicknesses, composite fibre orientation and damper location, has been in-

[☆]Please cite this article as: Aumjaud, P., Fieldsend, J.E., Boucher, M.-A., Evans, K.E., Smith, C.W., *Multi-objective optimisation of viscoelastic damping inserts in honeycomb sandwich structures*, *Composite Structures*, **119** (2015), 322-332, doi:<http://dx.doi.org/10.1016/j.compstruct.2015.05.061>

*Corresponding author. Tel.: +44(0)1392 723652

Email address: c.w.smith@exeter.ac.uk (C.W. Smith)

vestigated with various methods including genetic algorithms [12], cellular automata [13] or the method of moving asymptotes [14, 15]. Some of these optimised configurations for constrained layer dampers were investigated for honeycomb cored sandwich panels, and compared with solutions using DSLJ dampers. The DSLJ dampers were placed at locations with the highest strain energy in the first vibration mode [10]. The DSLJ damper was notable because it exhibited a better weight-efficient damping performance than the constrained layer dampers, i.e. the ratio of modal loss factor to mass was higher.

Implementation of heuristic optimisers to such problems can be a computationally expensive and difficult process. The question arises whether such methods are necessary or whether simpler approaches can yield similar quality results. In this paper, the location and orientation of DSLJ damper on a honeycomb-cored sandwich plate is optimised using two different approaches; (i) a quick and simple parametric optimisation based on the strain distribution of the mode shape of each structure considered, and (ii) a more complex and computationally demanding multi-objective evolutionary algorithm, namely the Adaptive Indicator-Based Evolutionary Algorithm (IBEA) [16]. The objective functions to be minimised are the negative of the modal loss factors and the total mass of the structure.

2. Methods

The approach taken here was to optimise the same structures with two approaches, a computationally simple and quick method and a more complex and computationally demanding method. As well as identifying new and highly weight-efficient damping configurations, this would identify whether the use of evolutionary optimisation methods would be required for similar problems. The structure chosen was a rectangular plate (aspect ratio of approximately 1.7), modelled in both cantilevered and free boundary conditions, and constructed as a sandwich panel with a honeycomb core.

The honeycomb core was composed of an array of 181 hexagonal cells, with 10 complete cells along its length and 10 complete cells across its width, plus 9×9 interleaving cells, see Figure 1. The sandwich plate was 300 mm long, 173 mm wide and 10 mm thick. The size of the panel was chosen so as to provide the subsequent optimisation with a large enough search space, while keeping the computational cost within reason. The cells were regular hexagons, with cell walls 10 mm long and 0.2 mm thick. The two sandwich skins were 0.2 mm thick and considered to be perfectly bonded to the core. The DSLJ damping insert is shown in Figure 2, and is formed by aluminium constraining layers sandwiching a viscoelastic lossy centre. There were three possible different orientations for the DSLJ within the honeycomb cell, see Figure 3. The DSLJ insert was offset by 1 mm from the top and the bot-

tom of the cell in order to prevent any contact between the insert and skin during flexure.

The sandwich structure was modelled using commercial finite element software (ANSYS 14.0) [17]. Four-node structural shell elements with six degrees of freedom per node (SHELL181 in ANSYS) were used to mesh the honeycomb core and skins. The viscoelastic material within the DSLJ was meshed with an eight-node brick element with three degrees of freedom per nodes (SOLID185 in ANSYS). A total of approximately 33 000 elements were used to mesh the sandwich structure. The nodes at the interface between the solid and the shell elements were forced to be coincident and their degrees of freedom were coupled in order to enforce compatibility between shell and solid elements. The enhanced strain formulation was used to prevent shear locking of the brick elements. The honeycomb and the sandwich skins were considered to be made of aluminium and the damping material in the DSLJ of a viscoelastic silicone rubber. The properties of the viscoelastic material were taken from Chia et al. [13] and were typical for a silicone rubber at constant room temperature. The aluminium's intrinsic loss factor was considered to be 0.0001 [18], set out with other relevant properties in Table 1. The material-dependant damping model was adopted in ANSYS to describe the damping ratio of the materials [19]. The sandwich plates were subjected to both cantilever and free boundary conditions. Specifically, the cantilever boundary condition consisted in constraining all degrees of freedom of all nodes at $x = 0$, i.e. sitting on the short edge of the panel, with all other nodes free. The free boundary condition imposed no constraints on any nodes. The eigenvalue problem, described in equation 1, is solved by modal superposition using the Preconditioned Conjugate Gradient (PCG) iterative solver and the first two modes were extracted using the Lanczos PCG modal extraction method:

$$(K - \omega^2 M)\phi = 0 \quad (1)$$

where K and M are the stiffness and mass matrices of the structure, respectively and ω and ϕ are the angular modal frequency and mode shape vector, respectively. The mode shapes are normalised with respect to the mass matrix. In the case of the free boundary conditions, the rigid body modes were not considered. The first two modes shapes for each boundary condition are illustrated in Table 2. The modal loss factors were computed using the Modal Strain Energy method [20] as described in equation 2,

$$\eta_i = \frac{\eta^{al} U_i^{al} + \eta^{vem} U_i^{vem}}{U_i^{al} + U_i^{vem}} \quad (2)$$

where η_i is the modal loss factor of mode i , η^{al} and η^{vem} are the material loss factors of the aluminium and the viscoelastic material, respectively. U_i^{al} and U_i^{vem} are the strain energies of mode i in the aluminium and the viscoelastic material, respectively and are calculated as fol-

low,

$$U_i = \frac{1}{2} \phi_i^T K \phi_i \quad (3)$$

where ϕ_i is the mode shape of mode i . This method is widely used for predicting the modal loss factor in structures composed of two or more different materials, although it is known that it is not the most accurate method and can tend to over-estimate modal loss factors especially for materials with a high loss factor [21]. However, its computational simplicity makes it much better suited for optimisation problems with a large number of evaluations, and since it was applied consistently in this study the results are at least comparable internally.

	Skins and honeycomb cells [18]	Viscoelastic material [13]
Density (kg/m ³)	2700	1100
Material loss factor	0.0001	0.3
Young's modulus	70 GPa	8.7 MPa
Poisson's ratio	0.3	0.45

Table 1: Material properties of the constituent materials of the DSLJ damper.

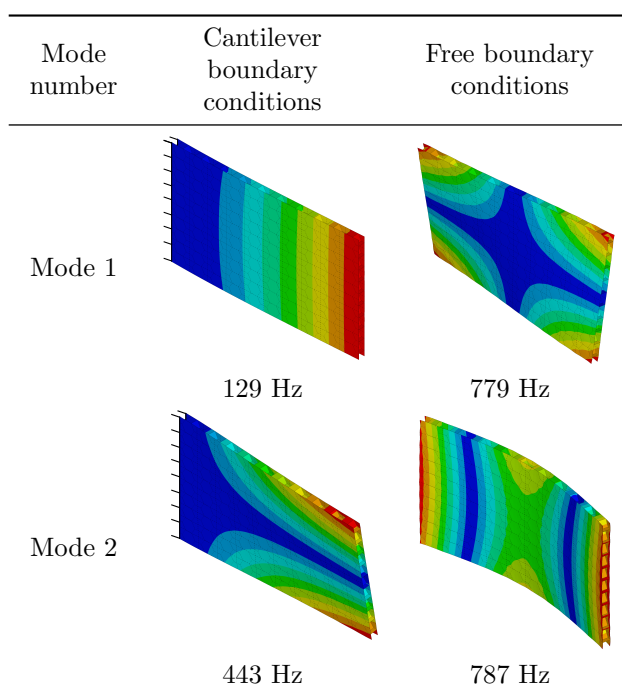


Table 2: First and second mode shapes of the sandwich plate under cantilever and free boundary conditions, along with their corresponding natural frequency. The colours on the mode shapes indicate the nodal displacements, with red being maximal and blue minimal. The encastered boundary condition is represented by black lines on the left of the cantilevered structures.

2.1. Parametric optimisation

As stated in the introduction, the objective of this study was to find the best locations and orientations of

the DSLJ dampers on the structure in order to achieve the highest damping for the least added mass. For this particular problem, there are four different possible damper configurations — absent or one of three orientations, and the structure is made of 181 cells. This makes a total of 4^{181} combinations or potential damper configurations; too large a solution space to evaluate every solution. The parametric optimisation method was based upon deformation data taken from the mode shape of a sandwich panel without any inserts, i.e. the empty panel. For each hexagonal cell in the empty panel core, the distance between two opposite corners was calculated in the undeformed and deformed cases. The percentage change in the corner-to-corner distance was ranked. DSLJ dampers were oriented and placed in the cells with maximum corner-to-corner deformations, in an attempt to ensure the highest possible strains. It was assumed that larger deformation in the DSLJ would result in higher energy dissipation and thus a higher modal loss factor than for dampers undergoing smaller deformations. This process was repeated iteratively, adding further DSLJ dampers until all cells were occupied. Sets of weight- and damping-efficient configurations could thus be identified for each of the cases considered here.

2.2. Adaptive IBEA optimisation

The general task for a multi-objective optimiser is to return a good estimate of the Pareto set of designs for a particular problem. That is, those designs for which it is impossible to improve performance on one objective, by varying its design parameters, without causing a degradation in performance one or more other quality measures. If we consider w.l.o.g. minimisation problems, then a legal design \mathbf{x}_1 is said to *dominate* another legal design \mathbf{x}_2 , denoted $\mathbf{x}_1 \prec \mathbf{x}_2$, iff $f_i(\mathbf{x}_1) \leq f_i(\mathbf{x}_2)$ for all objective functions $f_i(\cdot)$, and $\mathbf{f}(\mathbf{x}_1) \neq \mathbf{f}(\mathbf{x}_2)$. The Pareto set of designs is therefore defined as $\mathcal{P} = \{\mathbf{x} \in X \mid \exists \mathbf{u} \in \mathcal{X}, \mathbf{u} \prec \mathbf{x}\}$, where \mathcal{X} is the set of legal designs (those satisfying all equality and inequality constraints). Depending on the problem at hand, \mathcal{P} may be infinite in cardinality, and may be unknown.

Quality indicator functions are a means to assign a value to how good an estimated Pareto set is, either with respect to some (potentially unattainable) ideal performance (unary indicators), or in comparison to some other putative set (binary indicators) [22]. The Adaptive Indicator-Based Evolutionary Algorithm (IBEA), introduced by Zitzler and Künzli [16], is a modern multi-objective evolutionary algorithm, and one of the first to employ a quality indicator in its selection mechanism.

Although there are successful point-based optimisers for multi-objective design problems (e.g. simulated annealing [23]), using a set-based optimiser such as Adaptive IBEA has a number of benefits on this type of design problem. The recombination of designs that crossover provides allows the algorithm to make larger movements in design space, but within regions bounded by already ‘good’ solutions. Useful substrings in designs can thus be exploited,

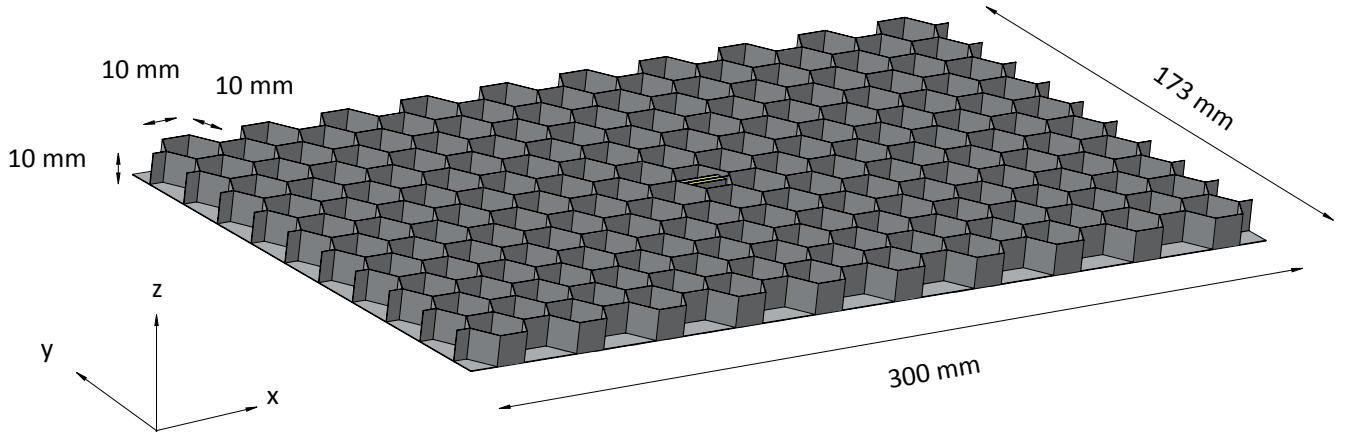


Figure 1: The array of hexagonal cells in the honeycomb core and the lower skin, with upper skin removed for clarity. A single DSLJ insert is sketched in the centre.

and disparate regions of design space can be optimised in parallel. The small refinement moves that point-based approaches are constrained to are also exploited in the mutation moves of a genetic algorithm, so this ability is not sacrificed. Furthermore, from a scalability standpoint, population-based optimisers are parallelised relatively easily, with the evaluation of each member fed to a different core, which enables computationally expensive optimisation problems to be tackled. Point-based approaches cannot be transferred as directly into parallel architectures.

Adaptive IBEA allows the embedding of user determined binary quality indicators to enable the comparison of designs maintained by the algorithm, enabling user preferences to be directly embedded within the search process, as long as the indicator is Pareto-compliant. In order to be Pareto-compliant, if one set approximation B can be said to be better than another set approximation A in a Pareto sense (that is, every member in A is dominated by, or equal to every member of B and $A \neq B$), then B should have a better indicator score [16].

Adaptive IBEA uses a binary indicator by exploiting it in the *fitness* assigned to each member (design) maintained by its search population, X . This fitness quantifies a design's contribution to the overall quality of the set of designs maintained by the optimiser, and is used to decide which designs to replace with newly evolved solutions as the search progresses. The fitness of a design \mathbf{x} , is calculated as:

$$F(\mathbf{x}) = \sum_{\mathbf{u} \in X \setminus \{\mathbf{x}\}} -e^{-I(\{\mathbf{u}\}, \{\mathbf{x}\})/c\kappa} \quad (4)$$

where c is the maximum absolute indicator value calculated across all members of X . κ is a term to scale the assigned fitnesses, we employ $\kappa = 0.05$ as in [16].

Here we use the popular additive epsilon indicator function, $I_{\epsilon+}(A, B)$, for the quality indicator term $I(\{\mathbf{u}\}, \{\mathbf{x}\})$ [22]. This quality indicator gives the minimum distance

required for one Pareto set approximation B to be translated (in objective space) in order for the approximation to weakly dominate another approximation, A . That is for the image in objective space of each member of A to be dominated by, or equal to, at least one member of the image in objective space of B . Formally, its calculation is:

$$I_{\epsilon+}(A, B) = \min_{\epsilon} \{ \forall \mathbf{b} \in B \ \exists \mathbf{a} \in A : f_i(\mathbf{a}) - \epsilon \leq f_i(\mathbf{b}) \} \quad (5)$$

for $i \in \{1, \dots, d\}$

for a d -objective problem. The Adaptive IBEA algorithm is presented in Algorithm 1.

Adaptive IBEA was implemented in the MATLAB numerical computing environment and invoked a commercial finite element code (ANSYS) in order to evaluate discrete models and compute their quality.

Overall six different cases were optimised. The sandwich plate was optimised for modes 1 and 2 under both cantilever and free boundary conditions, i.e. four cases. In these, the two objectives considered were the negative of the modal loss factor of the mode in question, and the percentage of additional mass on the structure. Two further cases consisted of optimising over three objectives: the negative of the first two modal loss factors as well as the additional mass in percent. The design parameters in our problem are the location and the orientation of the DSLJ damping inserts, which we represent in Adaptive IBEA as a 362-element long binary string, resulting in a search space cardinality of 2^{362} . A bit pair represents the different damper orientations (or no damper), with the location in the string of a particular bit pair determining the location in the sandwich plate it encodes.

Rather than initialising the optimiser search population with a random set of designs, we initialise its initial population with the $m = 20$ configurations identified by the parametric optimisation for the 2-objective optimisation. In the case of the 3-objective optimisation, the initial population was created as the union of the non-dominated

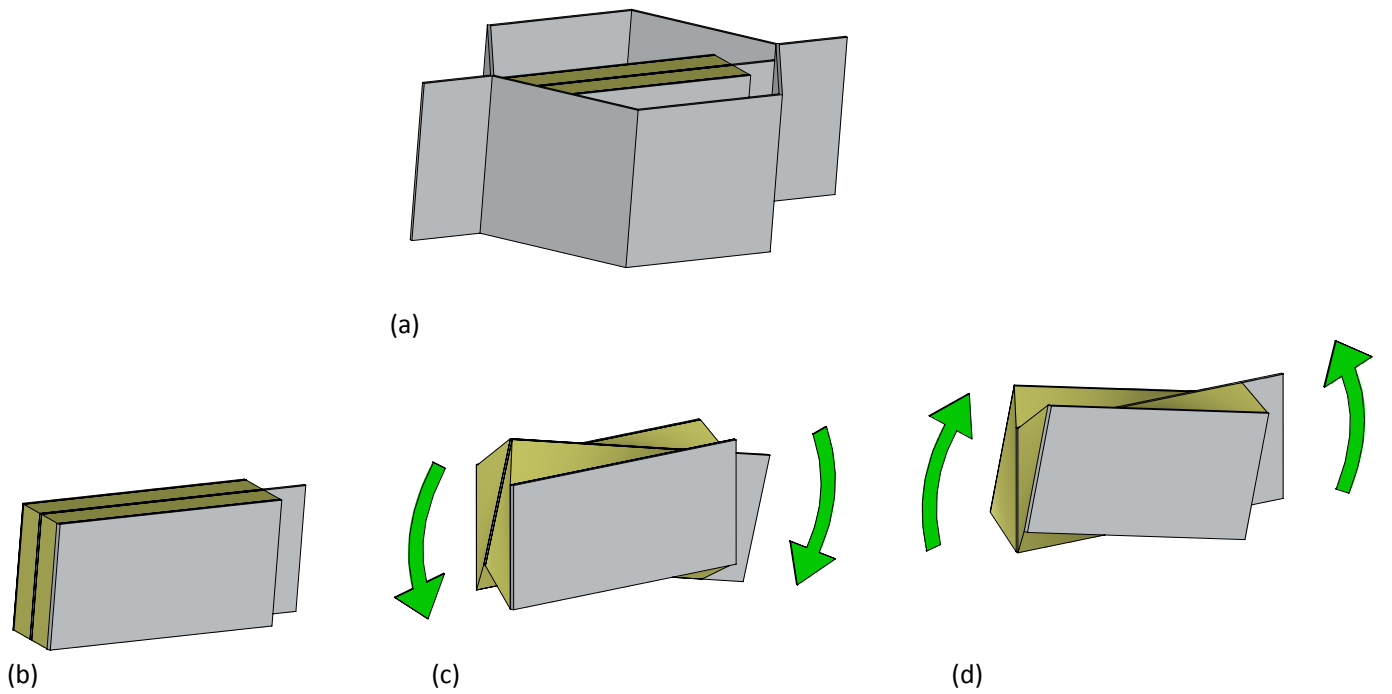


Figure 2: A hexagonal honeycomb cell with a DSLJ insert (a), a DSLJ insert alone (b), a DSLJ insert under deformation as might occur in flexure of the sandwich panel (shown exaggerated for clarity) in both directions (c) and (d). The yellow solid represents the viscoelastic, and the grey the constituent array material.

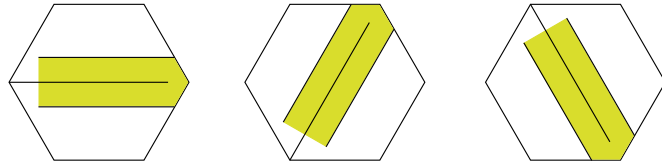


Figure 3: Three possible orientations of a DSLJ damper in a hexagonal cell.

solutions yielded by the two previous 2-objective optimisation. In this case, the population size was chosen to $m = 100$ to obtain a better populated estimated Pareto surface. At each algorithm iteration the objective values that are represented in X are scaled to the interval $[0, 1]$ and these scaled objectives are used to compute the indicator values (see equations 4 and 5) and the resultant fitness for each member of X .

The ‘environmental selection’ section of Adaptive IBEA (lines 9–13 of Algorithm 1) then progressively discards the less fit member of X in turn (recalculating the fitnesses of all remaining members of X each time) until the size of the population reaches m . A set of individuals X' (a mating pool) is filled by tournament selection between two randomly chosen individuals from X , with the fitter individual added to the mating pool X' . This is repeated until $|X| = |X'|$.

As well as employing standard evolutionary operators, we use an additional domain specific operator in the vary

subroutine (line 15). As standard, designs were evolved using uniform crossover of the binary string representation of two parent designs (with a probability of 0.9). The subsequent child solution was then mutated, with each string element having a $1/362$ probability of being flipped. When crossover is not used, then a single parent copy was instead subject to this mutation. This combination enables potentially large changes to designs via crossover, as well as ‘fine-tuning’ via mutation. We additionally introduce a *reflection* operator here, which was applied to 10% of designs after the mutation step. Intuitively we would expect that for a number of our problems an equal mass distribution with respect to the horizontal or vertical line of symmetry is likely to be advantageous. Our symmetric reflection operator provides a supply of these types of solution by generating children whose design is generated by folding an intermediate design’s left-hand cells through the line of vertical symmetry to assign the right-hand cells (or the reverse) or alternatively reflecting the top half to the bottom half (or vice versa). Any given design may therefore be converted via symmetric reflection to one of four reflected offspring, which will exhibit at least one line of symmetry. The optimiser was run for 1500 iterations (8.7 days) on a modern desktop machine with eight 16 GB RAM processors running in shared-memory parallel for each problem – meaning 30 000 designs were evaluated in an optimiser run. The 3-objective optimisation was only run for 50 iterations since its population size was bigger

Algorithm 1 The Adaptive IBEA of [16]

Require: m	Search population size
Require: N	Maximum number of iterations
Require: κ	Fitness scaling factor
Require: $I()$	Pareto-compliant binary indicator function
1: $X := \text{initialise}(m)$	Generate initial search population
2: $Y := \text{evaluate}(X)$	Evaluate objective values for members of X
3: $Y := \text{rescale}(Y)$	Rescale the objectives to range $[0, 1]$ using current bounds in Y
4: $F := \text{calculate_fitness}(X, I(), \kappa)$	
5: if termination_condition_met(N) then	
6: $A := \text{extract_non_dominated_members}(X)$	Extract Pareto set approximation
7: return A	Return designs in Pareto set approximation
8: end if	
9: while $ X > m$ do	
10: $x := \text{get_least_fit_design}(F, X)$	Identify least fit solution
11: $X := X \setminus \{x\}$	Remove least fit solution
12: $F := \text{calculate_fitness}(X, I(), \kappa)$	Update fitness of remaining
13: end while	
14: $X' := \text{copy}(X, X)$	Copy $ X $ solutions into X' using binary tournament selection
15: $X' := \text{vary}(X')$	Evolve new designs
16: $Y' := \text{evaluate}(X')$	Evaluate objective values for members of X'
17: $X := X \cup X'$	Merge the search population with the new designs
18: $Y := Y \cup Y'$	
19: goto 3.	Iterate algorithm

than the 2-objective case.

3. Results

3.1. Parametric optimisation

First the locations and orientations of the DSLJ dampers were optimised following the parametric approach. The results are presented in Figures 4 to 7, in each case the best solution (i.e. the one with the highest ratio of deformation:weight) is given on the left hand side, the fully filled solution on the right hand side, and an intermediate configuration in the middle. In the case of the cantilever plate, the best locations for DSLJ inserts tended to be near the clamped edge – see Figures 4 and 5. Under the first bending mode, the optimised orientations for DSLJ dampers were parallel to the long dimension of the plate, see Figure 4. Under the second mode which is a torsion mode, the optimised orientations for damping inserts were angled (at either $\pm 60^\circ$) to the long axis of the plate, as illustrated in Figure 5. For the sandwich plate under free boundary conditions, the better locations tend to be located near the centre of the plate. In the first mode the damping inserts are best when oriented radially outwards (see Figure 6), as opposed to the second mode where the best orientation tends to be a mix of axial and circumferential (see Figure 7). The orientation of the DSLJ inserts in the hexagonal cells seems to match the direction of the principal strains on the skin surface of the empty structure.

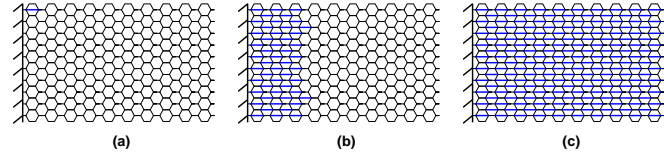


Figure 4: Optimised distributions of DSLJ dampers on the cantilever sandwich plate under mode 1 after the parametric optimisation – the optimised configuration (a), the fully filled plate (c) and an intermediate configuration (b) are shown.

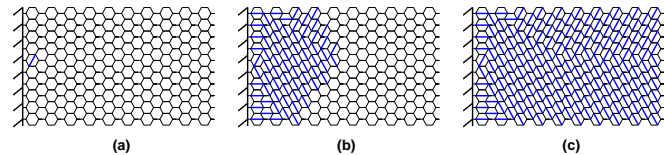


Figure 5: As per Figure 4 but for the cantilever sandwich plate under mode 2.

3.2. Adaptive IBEA optimisation

The results of the Adaptive IBEA optimisation are shown in Figures 8 to 15, with the added mass due to the DSLJ dampers shown *vs* the modal loss factor. The generation number in these Figures is indicated by colour, with blue being early and red being later. For all cases the initial population as well as non-dominated solutions are identified with filled points (see Figure legends). The configuration of one non-dominated solution for each case is sketched along with its mode shape. In the diagrams of

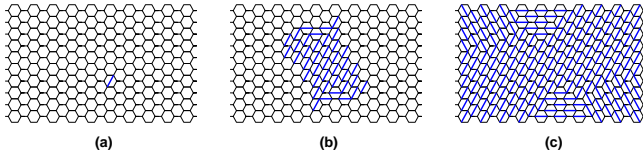


Figure 6: As per Figure 4 but for the free sandwich plate under mode 1.

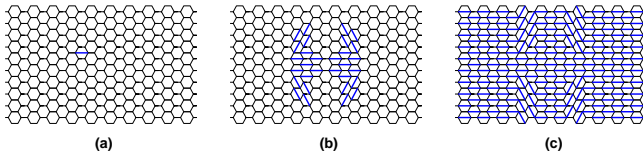


Figure 7: As per Figure 4 but for the free sandwich plate under mode 2.

the associated mode shapes, the maximal normalised displacement is indicated by red and the minimal with blue.

In common with the mode shapes, it can be noted that most of the cantilever non-dominated configurations are symmetrical with respect to the horizontal mid axis of the cantilever and similarly, in the case of the free boundary conditions most of the non-dominant configurations are symmetrical both vertically and horizontally, see Figures 9, 11, 13 and 15.

For the cantilever plate under its first bending mode, the initial population which was derived from the parametric optimisation and the non-dominated Adaptive IBEA solutions have similar objective values, as shown in Figure 8, and the two optimised configurations are also similar, see Figures 4 and 9. In contrast under the first torsional mode (mode 2), the non-dominated configurations are better than the initial population, see Figure 10. Specifically, the non-dominated solutions achieve up to 27% higher modal loss factors than the parametrically optimised configuration with a similar additional mass.

In the case of the free plate, an interesting phenomenon has occurred: the addition of 10 damping inserts has induced a swap in the order of the natural frequencies. Specifically, the erstwhile second mode (a bending mode originally at 787 Hz) had its frequency decline below the frequency of the erstwhile first mode (a torsional mode originally at 779 Hz), see Table 2. This lead to a wholly inadequate placement of the damping inserts in the parametric approach, and thus a poor damping efficiency, reaching a maximum loss factor of only 2.5×10^3 for a significant 70% increase in mass for the free sandwich plate originally optimised for its first mode. These mode swaps – or veering – occurring in the initial population are illustrated in Figure 12 and 14 by circle and diamond markers. In contrast Adaptive IBEA was able to identify much superior configurations appropriate to the new shape of the first mode, with a modal loss factor of up to 4.5×10^3 for only an 18% increase in mass with respect to the empty

structure. The Adaptive IBEA optimised configurations appear thoroughly different from the parametrically optimised configurations (the Adaptive IBEA's initial population), see Figure 13. A similar situation can be noted in the case of the free boundary condition plate optimised for its second mode, where four mode swaps can be identified as dampers were added to the structure in the parametric optimisation, see the diamond and circle markers in Figure 15. It is not surprising that Adaptive IBEA has determined significantly better configurations for this case; beating the initial population by more than sixfold in modal loss factor for a similar additional mass, see Table 3.

It is possible to optimise for more than one mode at a time. Here Adaptive IBEA was used to maximise simultaneously the first two modal loss factors and to minimise the added mass in a 3-objective optimisation. When modes are considered individually for both the cantilever or free plates, the 3-objective optimised solutions perform less well (i.e. they are heavier and less damped) than *vs* the 2-objective optimised solutions, see Figures 16 and 18. An attainment surface [24] was used to help visualising the approximation set more clearly in three dimensions. The distributions of inserts in the 3-objective optimised configurations appear to be combinations from the 2-objective configuration where modal loss factors were maximised individually, see Figures 17 and 19.

3.3. Parametric *vs* Adaptive IBEA optimisation

The results of the parametric and Adaptive IBEA optimisation are compared in Table 3, specifically the modal loss factors, mass and damping efficiencies for each configuration. The objectives (modal loss factors and mass) are normalised to those of the empty structure. The damping efficiency is defined as a criterion for comparing the different solutions, and is computed as the modal loss factor divided by the mass. As would be expected, all optimised configurations exhibited higher modal loss factors than the empty structure; reaching up to 43 times for the first modal loss factor η_1 in the Adaptive IBEA optimised cantilever case. These increases in loss factors come at the cost of moderate increases in mass, for example 21% additional mass for the Adaptive IBEA optimised cantilever case in mode 1. In the cantilever sandwich case optimised for mode 1, the damping efficiency is similar for both the parametric and Adaptive IBEA solution. However for all other cases, Adaptive IBEA outstrips the parametric approach, in particular for the free boundary condition cases where the damping efficiency after the Adaptive IBEA optimisation is about five and seven times higher than that of the parametric optimisation for mode 1 and 2, respectively.

4. Discussion

Both the parametric and Adaptive IBEA optimised configurations show better performance than the empty

Optimisation approach	Boundary conditions	η_1	η_2	Mass	Damping efficiency
Parametric	Cantilever	42.0	-	1.20	34.9
		-	12.5	1.29	9.74
	Free	8.55	-	1.16	7.35
		-	4.16	1.12	3.71
Adaptive IBEA	Cantilever	43.0	-	1.21	35.6
		-	15.6	1.27	12.3
		27.9	11.4	1.21	-
	Free	41.6	-	1.14	36.4
		-	32.2	1.13	28.6
		13.44	29.44	1.16	-

Table 3: Performance comparison between the parametric and Adaptive IBEA optimisation for the cantilever and free boundary condition cases. The configurations compared are identified by a magenta and a green point in Figs. 8 to 18 for the parametric and the Adaptive IBEA optimisation respectively. The mass m , the first η_1 and second η_2 loss factors are presented as a ratio of the empty structure. The damping efficiency, defined as the ratio η_1/m or η_2/m , is also indicated.

native structure, both in terms of absolute modal loss factors and damping efficiency, see Table 3. These two approaches are therefore relevant for this kind of problem. The DSLJ inserts placed following the parametric approach match the locations of maximum strain on the skin surface for the corresponding mode shape. For instance, the highest strains on the cantilevered plate is near the clamped edge for modes 1 and 2, and at the middle for a free plate, both of which correspond to the parametric configurations and orientations, see Figures 4 and 5. This agree with the placement of constrained layer damping treatments determined by the modal strain energy method, see for example [25]. The particular damping device used here is quite new, but the distributions of dampers identified and the suitability of the optimisation approaches may well be generic to any viscoelastic damper, or passive damper, or even active damper.

In the cantilever sandwich plate in its first mode, Adaptive IBEA and the parametric optimisation converged towards similar optimal solutions, meaning that there may only be one optimum solution and both approaches converged towards it, see Figure 8. Nevertheless, there are differences in all other cases, sometimes only subtle and sometimes more marked, e.g. see Figures 6 and 13. The differences in performance of these configurations however can be very large, e.g. the Adaptive IBEA configuration for the free plate which has a second modal loss factors up to an order of magnitude greater for a similar additional mass, see Figure 14. Thus, it appears that the parametric optimisation is less effective than the Adaptive IBEA optimisation in some if not all cases.

The reason for this is because the parametric optimisation does not account for the additional mass and stiffness which is inevitable when dampers are inserted, whereas the evolutionary optimisation implicitly does (as it affects the quality measures used to store and select designs). This has two consequences, (i) the strain energy distribution across the structure changes with additional mass and stiffness, ergo the optimal location and orientation of

DSLJ inserts changes, (ii) the additional mass and stiffness can cause veering, i.e. a change in the order of natural frequencies of modes, which can radically alter the efficacy of the dampers. The problem of veering is circumscribed by evolutionary optimisers such as Adaptive IBEA because it can simultaneously maximise loss factors and minimise mass for two or more modes, and thus the order of these modes does not affect the outcome. Hence structures prone to veering may benefit more from evolutionary optimisers which take veering into account, than from approaches like the parametric method herein which do not. Veering is more likely to happen when the natural frequencies of the modes are close, which is the case here for the free sandwich plate (779 Hz and 787 Hz for modes 1 and 2, respectively). It is well known that the mass of additional damping treatments may shift the natural frequencies towards lower values [26]. These frequency shifts may also be minimised by considering them as a penalty parameter in the evolutionary optimisation algorithms [12, 27, 28].

Unlike the parametric approach, Adaptive IBEA is capable of minimising more than two objectives simultaneously. Here, the 3-objective optimisation, specifically mass and the first two modal loss factors, yielded an evident trade-off between the two 2-objective solutions, see Figures 16 and 18. The 3-objective compromise solution retains a substantial global damping, with a significant penalty in some regions of the estimated Pareto front as is shown on the attainment surfaces. This may be particularly useful for structures subjected to excitations covering a wide range of frequencies, such as the compressor blades of a gas turbine subjected to an unsteady airflow [29].

Figure 16 indicates that there is a gentle rate of change in the estimated Pareto front in the region near to the green data point, and very steep gradients adjacent to the edge concerned with mode 2 and mass. This steep slope indicates that for a small sacrifice in loss factor for mode 2, a large gain can be made in loss factor for mode 1 in this region. In contrast Figure 18 indicates that there is no large difference in the rate of change of the estimated

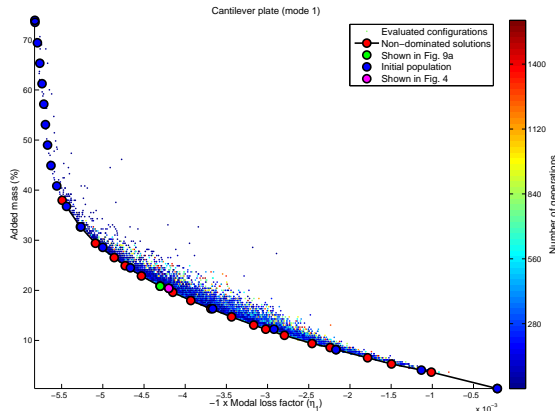


Figure 8: Cantilever sandwich plate - the initial population, the non-dominated solutions and all the evaluated configurations are represented by the negative of their first modal loss factor and their percentage of additional mass.

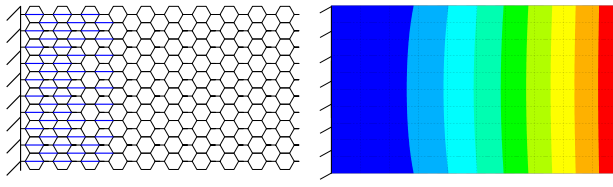


Figure 9: Optimised IBEA configuration for the cantilever plate under its first mode (a). This configuration corresponds to the green point in Figure 8. The corresponding mode shape of the empty structure, where the colour indicate the nodal displacements, with red being maximal and blue minimal (b).

Pareto front, so no region of the front is more stable than any other.

The particular parametric optimisation approach adopted here is quite efficient, requiring only one initial finite element evaluation. In this case, we also made a few more evaluations to generate a small initial population for the Adaptive IBEA algorithm. This stands in comparison to the 30 000 designs evaluated by the Adaptive IBEA optimisation. In general evolutionary optimisations are more computationally expensive and time consuming than parametric optimisations. However in this case, it was possible to constrain the parametric optimisation to a relatively small solution space, generated by the intracellular strain data. If it is not possible to do this, parametric optimisation can require enormous computational power, for instance if we considered all possible combinations of damper orientation and cell location for many modes.

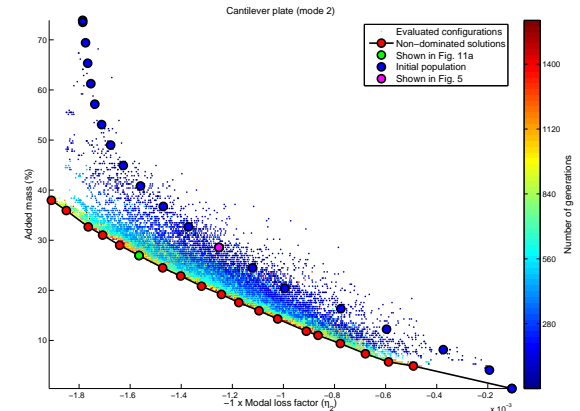


Figure 10: Cantilever sandwich plate - the initial population, the non-dominated solutions and all the evaluated configurations are represented by the negative of their second modal loss factor and their percentage of additional mass.

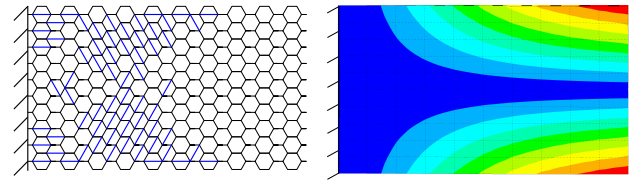


Figure 11: Optimised IBEA configuration for the cantilever plate under its second mode (a). This configuration corresponds to the green point in Figure 10. The corresponding mode shape of the empty structure, where the colour indicate the nodal displacements, with red being maximal and blue minimal (b).

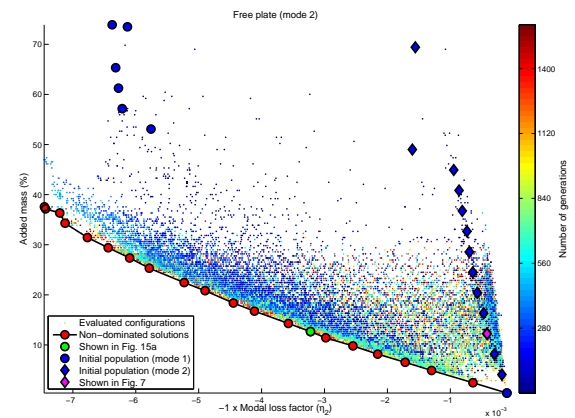
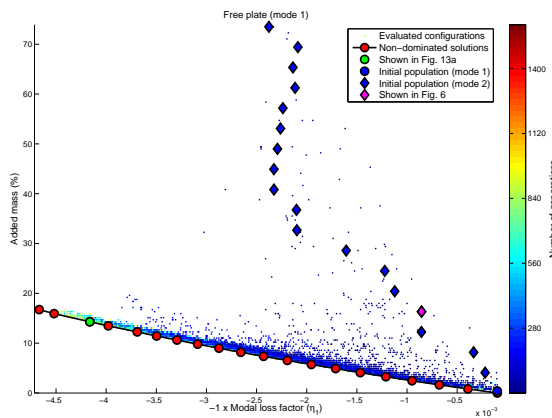
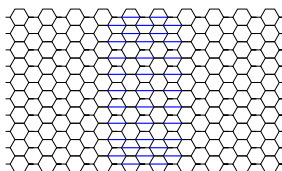
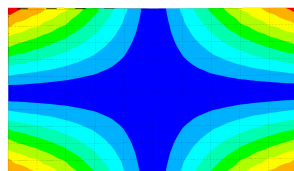


Figure 12: Free sandwich plate - the initial population, the non-dominated solutions and all the evaluated configurations are represented by the negative of their first modal loss factor and their percentage of additional mass. The initial population features two different mode shapes, represented by either a circle or a diamond.



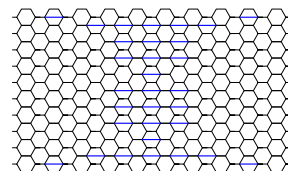
(a) Optimised configuration



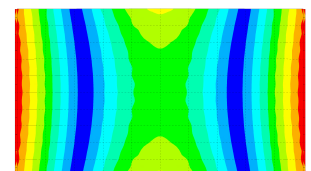
(b) Mode shape 1

Figure 13: Optimised configuration for the free plate under its first mode (a). This configuration corresponds to the green point in Figure 12. The corresponding mode shape of the empty structure, where the colour indicate the nodal displacements, with red being maximal and blue minimal (b).

Figure 14: Free sandwich plate - the initial population, the non-dominated solutions and all the evaluated configurations are represented by the negative of their second modal loss factor and their percentage of additional mass. The initial population features two different mode shapes, represented by either a circle or a diamond.



(a) Optimised configuration



(b) Mode shape 2

Figure 15: Optimised configuration for the free plate under its second mode (a). This configuration corresponds to the green point in Figure 14. The corresponding mode shape of the empty structure, where the colour indicate the nodal displacements, with red being maximal and blue minimal (b).

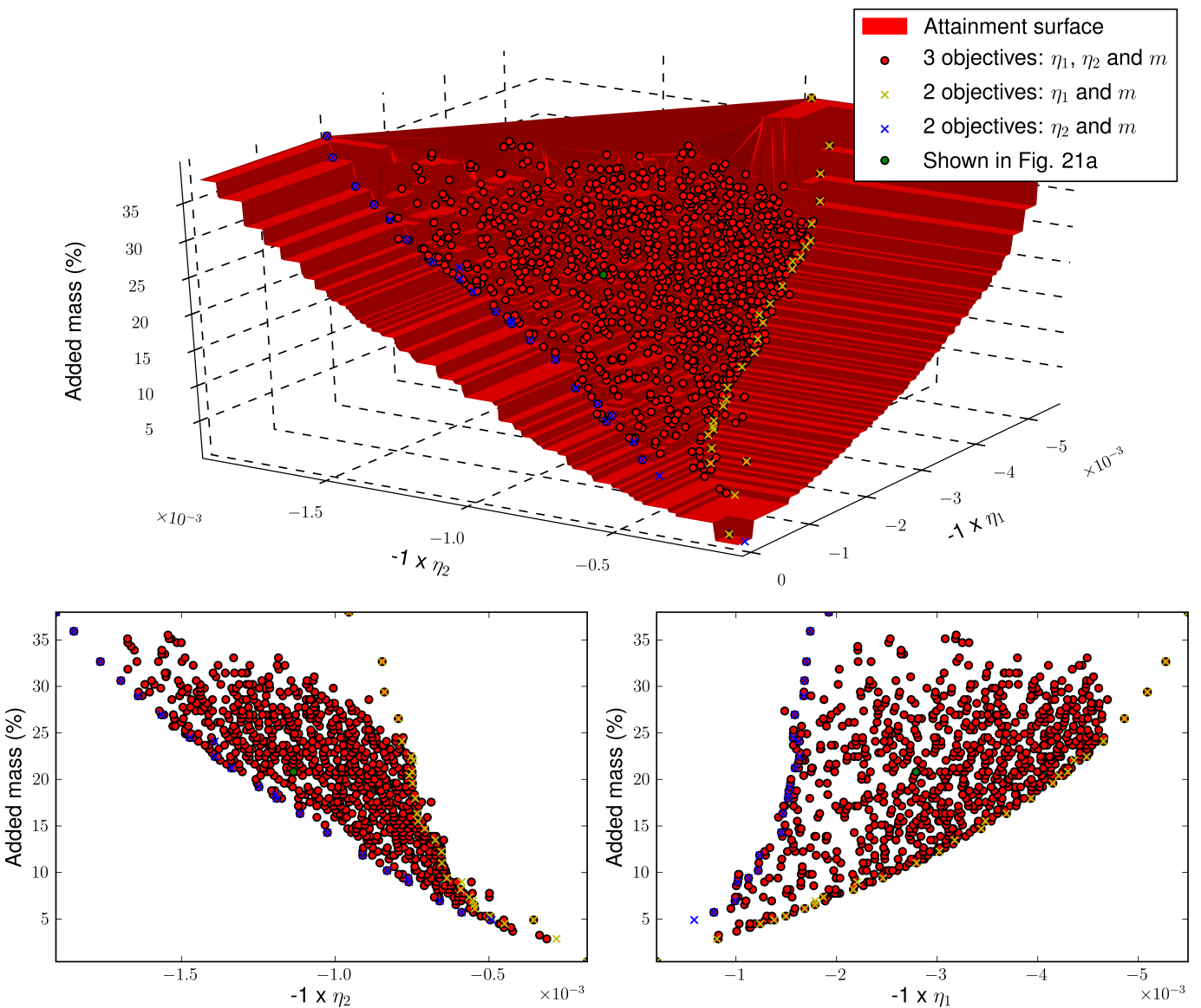


Figure 16: Cantilever sandwich plate - The non-dominated solutions, represented on an attainment surface, when the added mass and the negative of the first two modal loss factors are minimised simultaneously. The 3-objective and 2-objective solutions are compared on two projection plots.

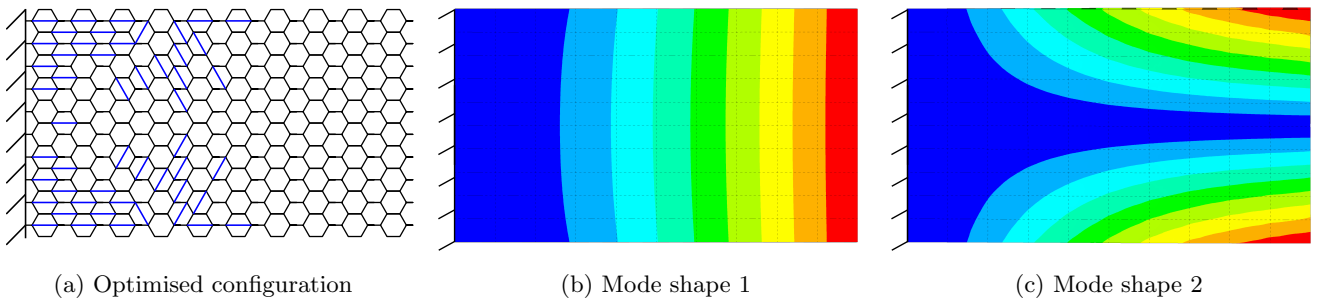


Figure 17: Optimised configuration for the free plate under its first and second mode (a). This configuration corresponds to the green point in Figure 16. The corresponding mode shape of the empty structure, where the colour indicate the nodal displacements, with red being maximal and blue minimal (b).

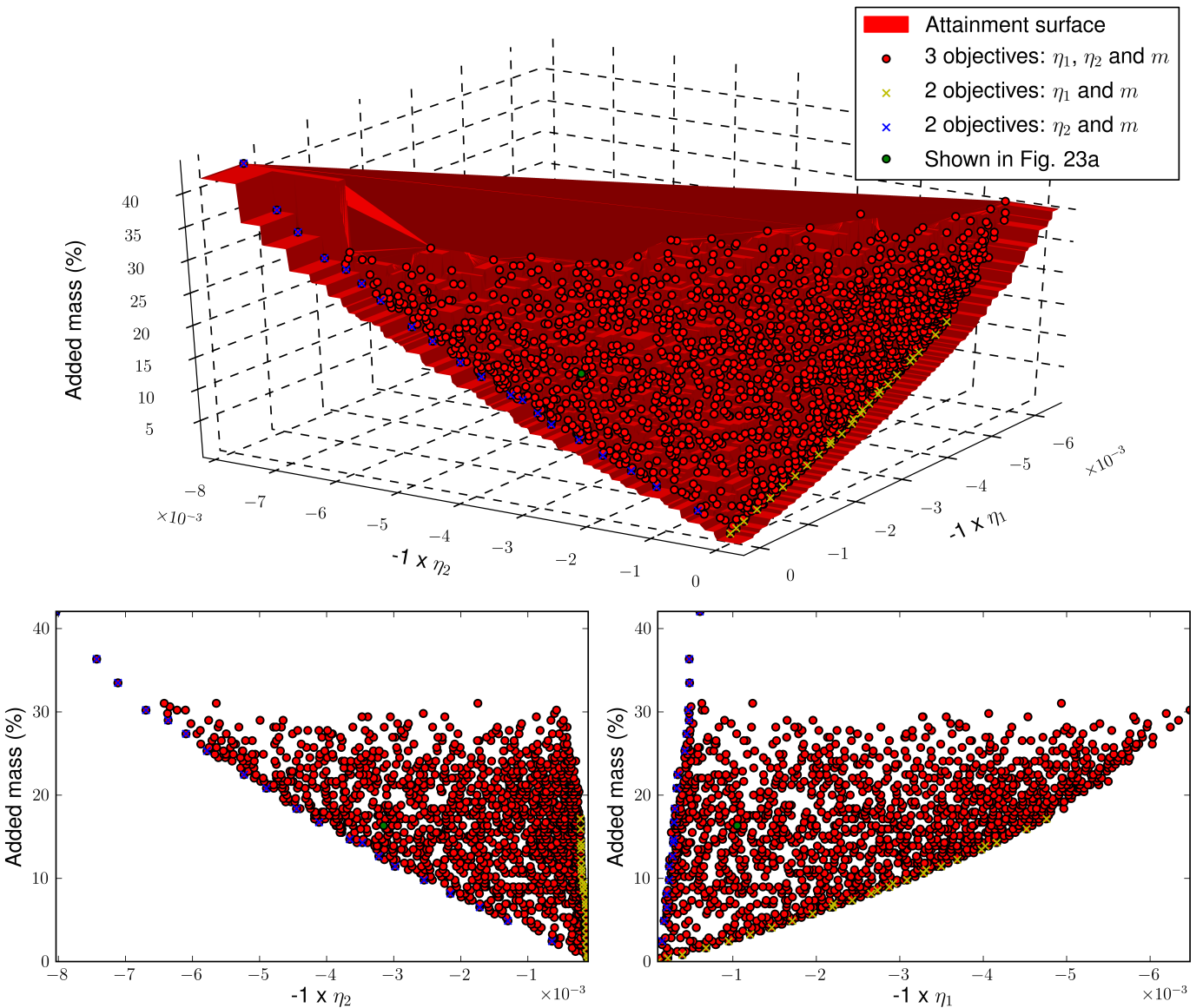


Figure 18: Free sandwich plate - The non-dominated solutions, represented on an attainment surface, when the added mass and the negative of the first two modal loss factors are minimised simultaneously. The 3-objective and 2-objective solutions are compared on two projection plots.

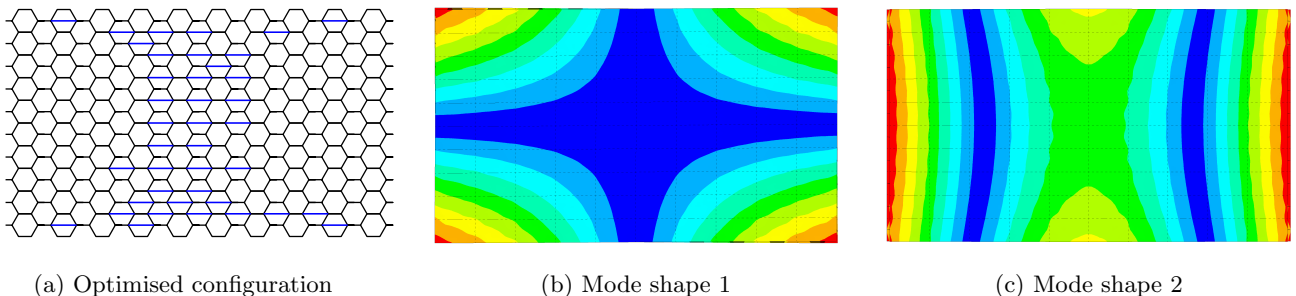


Figure 19: Optimised configuration for the free plate under its first and second mode (a). This configuration corresponds to the green point in Figure 18. The corresponding mode shape of the empty structure, where the colour indicate the nodal displacements, with red being maximal and blue minimal (b).

5. Conclusion

For the first time a study of the Double Shear Lap Joint damper has identified optimal weight-efficient configurations for honeycomb-cored sandwich plates with various boundary conditions. For example, the free sandwich plate was only made 13% heavier and produced a 32 times higher second modal loss factor than the empty structure after the Adaptive IBEA optimisation. On the other hand, the parametric approach yielded a configuration with only a 4 times greater modal loss factor for an equivalent increase in mass. In the present cases, the parametric approach is easier to implement and less computationally expensive than the Adaptive IBEA approach, and can be used to obtain a quick idea of the solution. However, the parametric approach does not take into account the change in mode shape nor the modal frequency shift due to the addition of the dampers. When neighbouring modes are close in frequency, such frequency shifts may well cause mode swaps (or veering) which is difficult to predict *a priori*. In such cases, the parametric approach places and orients the dampers in an inadequate manner, which severely detracts from their efficiency. In contrast, Adaptive IBEA can account for the effect of the addition of the damper because it minimises the mass and the modal loss factors directly, without assuming any relation between the corner-to-corner deformation and the damping. It is thus a more robust and reliable optimisation strategy than the parametric approach. Finally, Adaptive IBEA is a multi-objective optimisation algorithm capable of minimising the modal loss factors of a large number of modes simultaneously, which can be an interesting property for structures subjected to a wide range of excitation frequencies.

Acknowledgements

This work was supported by the MEET project (Material for Energy Efficiency in Transport) in the context of the INTERREG IV-A France (Channel) England European cross-border co-operation programme, which is co-financed by the ERDF.

References

- [1] L. J. Gibson, M. F. Ashby, *Cellular Solids: Structure and Properties*, Cambridge University Press, 1999.
- [2] D. Zenkert, *Handbook of Sandwich Construction*, EMAS, 1997.
- [3] Z. Li, M. J. Crocker, A Review on Vibration Damping in Sandwich Composite Structures, *International Journal of Acoustics and Vibration* 10 (4) (2005) 159–169.
- [4] E. M. Kerwin, Damping of Flexural Waves by a Constrained Viscoelastic Layer, *The Journal of the Acoustical Society of America* 31 (7) (1959) 952–962. [doi:10.1121/1.1907821](https://doi.org/10.1121/1.1907821).
- [5] D. Ross, E. Ungar, E. Kerwin, Damping of plate flexural vibrations by means of viscoelastic laminae, *Structural Damping* (1960) 49 – 87.
- [6] D. Nokes, F. Nelson, Constrained layer damping with partial coverage, *The shock and vibration bulletin* 68 (part 3) (1968) 5 – 12.
- [7] G. Michon, A. Almajid, G. G. Aridon, Soft hollow particle damping identification in honeycomb structures, *J. Sound Vibr.* 332 (3) (2013) 536–544. [doi:10.1016/j.jsv.2012.09.024](https://doi.org/10.1016/j.jsv.2012.09.024).
- [8] G. Murray, F. Gandhi, E. Hayden, Polymer-filled honeycombs to achieve a structural material with appreciable damping, *J. Intell. Mater. Syst. Struct.* 23 (6) (2012) 703–718. [doi:10.1177/1045389X12439636](https://doi.org/10.1177/1045389X12439636).
- [9] M.-A. Boucher, C. W. Smith, F. Scarpa, R. Rajasekaran, K. E. Evans, Effective topologies for vibration damping inserts in honeycomb structures, *Composite Structures* 106 (2013) 1–14. [doi:10.1016/j.compstruct.2013.05.036](https://doi.org/10.1016/j.compstruct.2013.05.036).
- [10] P. Aumjaud, C. W. Smith, K. E. Evans, A novel viscoelastic damping treatment for honeycomb sandwich structures, *Composite Structures* 119 (2015) 322–332. [doi:10.1016/j.compstruct.2014.09.005](https://doi.org/10.1016/j.compstruct.2014.09.005).
- [11] R. Rajasekaran, M.-A. Boucher, F. Scarpa, K. Evans, Vibration damping, Patent US20130264757 A1 (Oct. 2013).
- [12] M. A. Trindade, Optimization of passive constrained layer damping treatments applied to composite beams, *Latin American Journal of Solids and Structures* 4 (1) (2007) 19–38.
- [13] C. M. Chia, J. A. Rongong, K. Worden, Strategies for using cellular automata to locate constrained layer damping on vibrating structures, *J. Sound Vibr.* 319 (1-2) (2009) 119–139. [doi:10.1016/j.jsv.2008.06.023](https://doi.org/10.1016/j.jsv.2008.06.023).
- [14] Z. Ling, X. Ronglu, W. Yi, A. El-sabbagh, Topology optimization of constrained layer damping on plates using Method of Moving Asymptote (MMA) approach, *Shock and Vibration* 18 (1) (2011) 211–244.
- [15] W. Zheng, Y. Lei, S. Li, Q. Huang, Topology optimization of passive constrained layer damping with partial coverage on plate, *Shock Vib.* 20 (2) (2013) 199–211. [doi:10.3233/SAV-2012-00738](https://doi.org/10.3233/SAV-2012-00738).
- [16] E. Zitzler, S. Kunzli, Indicator-based selection in multiobjective search, in: X. Yao, E. Burke, J. A. Lozano, J. Smith, J. J. MereloGuervos, J. A. Bullinaria, J. Rowe, P. Tino, A. Kaban, H. P. Schwefel (Eds.), *Parallel Problem Solving from Nature - Ppsn VIII*, Vol. 3242, Springer-Verlag Berlin, Berlin, 2004, pp. 832–842.
- [17] Ansys Mechanical APDL release 14.0, Theory Reference Manual, ANSYS, Inc.
- [18] S. S. Rao, *Mechanical vibrations*, 5th Edition, Prentice Hall, Upper Saddle River, N.J., 2011.
- [19] G. Lepoittevin, G. Kress, Optimization of segmented constrained layer damping with mathematical programming using strain energy analysis and modal data, *Mater. Des.* 31 (1) (2010) 14–24. [doi:10.1016/j.matdes.2009.07.026](https://doi.org/10.1016/j.matdes.2009.07.026).
- [20] C. D. Johnson, D. A. Kienholz, Finite Element Prediction of Damping in Structures with Constrained Viscoelastic Layers, *AIAA Journal* 20 (9) (1982) 1284–1290.
- [21] F. P. Landi, F. Scarpa, J. A. Rongong, G. Tomlinson, Improving the modal strain energy method for damped structures using a dyadic matrix perturbation approach, *Proc. Inst. Mech. Eng. Part C-J. Eng. Mech. Eng. Sci.* 216 (12) (2002) 1207–1216. [doi:10.1243/095440602321029445](https://doi.org/10.1243/095440602321029445).
- [22] J. Knowles, L. Thiele, E. Zitzler, A Tutorial on the Performance Assessment of Stochastic Multiobjective Optimizers, Tech. rep., Computer Engineering and Networks Laboratory (TIK), ETH Zurich, Switzerland (2006).
- [23] K. I. Smith, R. M. Everson, J. E. Fieldsend, C. Murphy, R. Misra, Dominance-Based Multi-Objective Simulated Annealing, *IEEE Transactions on Evolutionary Computation* 12 (3) (2008) 323–342.
- [24] J. Knowles, A summary-attainment-surface plotting method for visualizing the performance of stochastic multiobjective optimizers, in: 5th International Conference on Intelligent Systems Design and Applications (ISDA'05), IEEE, 2005, pp. 552–557. [doi:10.1109/ISDA.2005.15](https://doi.org/10.1109/ISDA.2005.15).
- [25] R. A. S. Moreira, J. D. Rodrigues, Partial constrained viscoelastic damping treatment of structures: A modal strain energy approach, *Int. J. Struct. Stab. Dyn.* 6 (3) (2006) 397–411. [doi:10.1142/S0219455406002003](https://doi.org/10.1142/S0219455406002003).

- [26] H. Panossian, Optimized Non-Obstructive Particle Damping (NOPD) Treatment for Composite Honeycomb Structures, in: 47th AIAA/ASME/ASCE/AHS/ASC Structures, Structural dynamics and material conference, 2006.
- [27] M. A. Trindade, Optimization of sandwich/multilayer viscoelastic composite structure for vibration damping, Vol. 3, 2001, pp. 257–264.
- [28] Y.-C. Chen, S.-C. Huang, An optimal placement of CLD treatment for vibration suppression of plates, International Journal of Mechanical Sciences 44 (8) (2002) 1801–1821. [doi:10.1016/S0020-7403\(02\)00042-5](https://doi.org/10.1016/S0020-7403(02)00042-5).
- [29] Rolls-Royce Ltd, The Jet Engine, Rolls-Royce, Derby, England, 1986.